JCTC Journal of Chemical Theory and Computation

Investigation of the Ligand-Field States of the Hexaammine Cobalt(III) Ion with Quantum Chemical Methods

François P. Rotzinger*

Institut des Sciences et Ingénierie Chimiques (ISIC), Ecole Polytechnique Fédérale de Lausanne (EPFL), Station 6, CH-1015 Lausanne, Switzerland

Received January 27, 2009

Abstract: The ligand-field (LF) transition energies of the $Co(NH_3)_6^{3+}$ ion have been computed with multiconfiguration quasidegenerate second-order perturbation theory (MCQDPT2). The water solvent was treated with the polarizable continuum model (PCM), and the environment in crystals was modeled by the $Co(NH_3)_6 \cdot Cl_4^-$ complex. The Co−N bond lengths, calculated for the hydrated cation and the $Co(NH_3)_6 \cdot Cl_4^-$ model compound, agree with those in the crystal structures. The vertical transition energies agree with experiment, whereby those based on $Co(NH_3)_6 \cdot Cl_4^-$ are more accurate than those for the hydrated ion. The 0−0 transitions were based on the OPBE geometries of ground and excited $^1T_{1g}$, $^3T_{1g}$, $^5T_{2g}$ states of the hydrated ion. The $^3T_{1g}$ state is the lowest excited state; the $^5T_{2g}$ state lies higher by >0.6 eV.

Introduction

For the understanding of the photochemical reactivity of hexaammine cobalt(III) complexes, it is desirable to know which excited state is lowest, the $^3T_{1g}$ or the $^5T_{2g}$ ligand-field (LF) state. Their geometries and, therefore, also their reactivities differ. In a low-temperature (8 K) electron spectroscopic study of the hexaammine cobalt(III) ion, the 0−0 transition energies to the lowest singlet ($^1T_{1g}$) and triplet ($^3T_{1g}$) LF states were determined.[1] The spectroscopically unmeasurable quintet state ($^5T_{2g}$) was proposed to lie below or at the same energy as the $^3T_{1g}$ state.[1] Later, in a theoretical treatment of the electron self-exchange reaction of the $Co(NH_3)_6^{2+/3+}$ couple, the energy of the relaxed $^5T_{2g}$ state was found to be higher than those of the $^1T_{1g}$ and $^3T_{1g}$ states according to ZINDO calculations.[2] On the basis of the excited state dynamics of three cobalt(III) complexes with chelating ligands, the $^5T_{2g}$ state was suggested to be the lowest LF state.[3]

Experimental LF transition energies of $Co(NH_3)_6^{3+}$ were measured in aqueous solution[4] and in the solid state,[1] in which the cation is surrounded by water or anions. In this study, the vertical and the 0−0 LF transition energies were investigated with quantum chemical methods by taking into account environmental effects.

* To whom correspondence should be addressed. E-mail: francois.rotzinger@epfl.ch.

Computational Details

The calculations were performed using the GAMESS[5,6] programs. For cobalt, the relativistic effective core potential (ECP) basis set of Stevens et al. (SBKJ)[7] was used. For chlorine, the ECP basis set of Stevens et al.[8] supplemented with a polarization function ($\alpha_d = 0.65$[9]) was taken. For N and H, the 6-31G(d) basis set[10,11] was used ($\alpha_d = 1.00$[9]). Some calculations were performed with tripleζ + polarization basis sets, 6-311G(d) for N and H,[12] and the outermost s and p functions of the SBKJ basis set were uncontracted (SBKJu). Figures 1 and 2 were generated with MacMolPlt.[13]

Hydration was treated using the polarizable continuum model (PCM).[14,15] The cavity was constructed based on the van der Waals radii of the atoms, whereby for cobalt, a value of 2.20 Å was taken. Because of the high charge of $Co(NH_3)_6^{3+}$, a finer tesselation than the default had to be used (NTSALL = 960, the default is 60; in PCM, each atom is represented by a sphere, which is approximated by NTSALL triangles). The DFT calculations were performed with a grid finer (NTHE = 24 and NPHI = 48) than the default (NTHE = 12 and NPHI = 24). The active space for the multiconfiguration quasidegenerate second-order pertur-

10.1021/ct900048r CCC: $40.75
Published on Web 03/26/2009

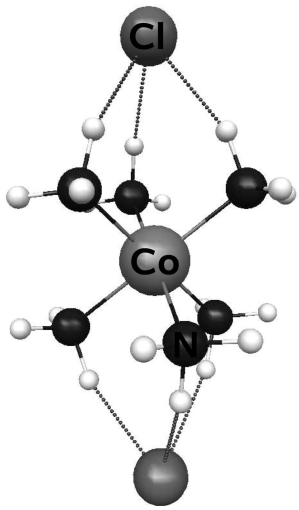

Figure 1. Perspective view of the $Co(NH_3)_6 \cdot Cl_2^+$ ion (MP2 geometry).

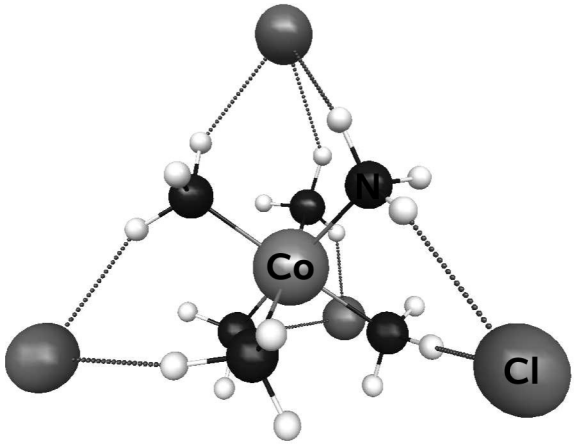

Figure 2. Perspective view of the $Co(NH_3)_6 \cdot Cl_4^-$ ion (OPBE geometry).

bation (MCQDPT2)[16,17] computations was determined via configuration interaction (CI) singles-doubles calculations.[18] A 10 electrons in 10 orbitals (10/10) active space was used for most MCQDPT2 calculations, whereby for each degenerate state, a state-averaged complete active space self-consistent field (CAS-SCF) calculation was performed. Since the symmetries of $Co(NH_3)_6^{3+}$, $Co(NH_3)_6 \cdot Cl_2^+$, and $Co(NH_3)_6 \cdot Cl_4^-$ are lower than O_h, the triply degenerate states split into an A and an E state. The CAS-SCF and the MCQDPT2 calculations were performed by averaging over the A and E states corresponding to the T state of interest. Hydration at the MCQDPT2 level was computed as described elsewhere.[19] Unless noted otherwise, only the 1s MOs of N were treated as frozen cores. Spin−orbit coupling was computed on the basis of the corresponding CAS-SCF wave function via spin−orbit CI with the full Breit−Pauli Hamiltonian including a partial two electron operator.[20−22] Interactions of each state with the others exhibiting the same symmetry and spin or a spin differing by ±1 were taken into account.

The geometry optimizations of the excited states $^1T_{1g}$, $^3T_{2g}$, and $^5T_{2g}$ with PCM hydration were performed at the spin unrestricted level (without spin projection). To achieve SCF convergence, orbital interchanges were restricted (restrct =.t. option in $scf), and level shifting or damping of the Fock matrix was applied (shift =.t. or damp =.t. option). The atomic coordinates of the $^1A_{1g}$, $^1T_{1g}$, $^3T_{2g}$, and $^5T_{2g}$ states of $Co(NH_3)_6^{3+}$ are given in Tables S1−S4 (Supporting Information), and those of $Co(NH_3)_6 \cdot Cl_4^-$ in its ground state are reported in Table S5 (Supporting Information).

Table 1. Co−N Bond Lengths from X-ray Crystal Structures

compound	*d*(Co−N), Å	reference
$[Co(NH_3)_6]_2[Ni(CN)_4]_3 \cdot 2H_2O$	1.964	23
$[Co(NH_3)_6][Co(CN)_6]$	1.97	24
$[Co(NH_3)_6]I_3$	1.96 ± 0.02	25
$[Co(NH_3)_6][ZnCl_4]Cl$	1.967	26
$[Co(NH_3)_6][FeCl_6]$	1.965	27
$[Co(NH_3)_6][SbCl_6]$	1.983	28
$[Co(NH_3)_6][Sb_2F_9]$	1.990 ± 0.005	29
$[Co(NH_3)_6][BrO_3]_3 \cdot {}^1/_2H_2O$	1.959	30
$[Co(NH_3)_6]Cl_2[BF_4]$	1.955	31
$[Co(NH_3)_6]Cl[SiF_6] \cdot 2H_2O$	1.965 ± 0.002	32

Results

Ground State Geometry of $Co(NH_3)_6^{3+}$. The Co−N bond lengths in the crystal structures, reported in Table 1, lie in the range of 1.96 −1.97 Å. The diversity of the anions in the crystals gives rise to different hydrogen bonds with the ammonia ligands. This is the reason why the Co−N bond lengths of the various compounds vary somewhat. Through these H bonds charge is donated to the cation. This strengthens the Co−N bonds compared with the free $Co(NH_3)_6^{3+}$ ion (in the gas phase). The quantum chemically determined Co−N bond lengths in free $Co(NH_3)_6^{3+}$, exhibiting D_3 symmetry, are summarized in Table 2. The Co−N bond lengths vary slightly upon improvement of the basis set from doubleζ + polarization to tripleζ + polarization. The Hartree−Fock (HF) method, neglecting electron correlation, produces too long Co−N bonds whereas MP2, neglecting static electron correlation, yields too short Co−N bonds. With CAS-SCF, neglecting dynamic electron correlation, too long Co−N bonds are obtained. The most accurate Co−N bonds are computed with MCQDPT2(10/10) which takes into account static and dynamic electron correlation. In the MCQDPT2(4/4) calculation with a smaller active space, a part of the static correlation is neglected, which leads to too short Co−N bonds as with MP2. The widely applied BLYP[33−35] and B3LYP[36−38] functionals gave rise to too long Co−N bonds. The PBE[39,40] and PBE0[41] functionals are superior. The OPBE[39,40,42] and OLYP[42] functionals exhibit the OPTX[42] exchange, which is superior to other exchange functionals.[43] OLYP yielded too long Co−N bonds. The best geometries with respect to MCQDPT2(10/10) were obtained with PBE0 and OPBE. For the $Co(NH_3)_6^{3+}$ complexes, these two functionals were assumed to provide the most accurate geometries.

The LF spectrum of the free $Co(NH_3)_6^{3+}$ ion (in the gas phase) is unknown. For comparison with the vis spectra in the solid state,[1] the environment of the cation was modeled by adding two or four chloride ions in the second coordination sphere. $Co(NH_3)_6 \cdot Cl_2^+$ (Table 2ii) exhibits

Table 2. Bond Lengths in $Co(NH_3)_6^{3+}$, $Co(NH_3)_6 \cdot Cl_2^{+}$, and $Co(NH_3)_6 \cdot Cl_4^{-}$ Computed with Various Methods and Basis Sets

method	basis set	d(Co−N), Å	d(N−H), Å
	(i) $Co(NH_3)_6^{3+}$, D_3 Symmetry		
HF	SBKJ/6-31G(d)	2.045	1.010
HF	SBKJ/6-311G(d)	2.042	1.006−1.007
HF	SBKJu/6-311G(d)	2.041	1.006−1.007
MP2[a]	SBKJ/6-31G(d)	1.986	1.025
MP2[b]	SBKJ/6-31G(d)	1.974	1.025−1.026
MP2[a]	SBKJ/6-311G(d)	1.981	1.021
MP2[b]	SBKJ/6-311G(d)	1.966	1.021
CAS-SCF(10/10)	SBKJ/6-31G(d)	2.034	1.009
CAS-SCF(10/7)	SBKJ/6-31G(d)	2.052	1.009−1.010
CAS-SCF(4/4)	SBKJ/6-31G(d)	2.047	1.009
MRMP2(10/10)[b]	SBKJ/6-31G(d)	2.014	1.027
MRMP2(4/4)[b]	SBKJ/6-31G(d)	1.997	1.025−1.026
BLYP	SBKJ/6-31G(d)	2.060	1.034−1.035
B3LYP	SBKJ/6-31G(d)	2.033	1.026
PBE	SBKJ/6-31G(d)	2.028	1.034
PBE0	SBKJ/6-31G(d)	2.006	1.024
OPBE	SBKJ/6-31G(d)	2.021	1.026
OLYP	SBKJ/6-31G(d)	2.052	1.027−1.028
	(ii) $Co(NH_3)_6 \cdot Cl_2^{+}$, D_{3d} Symmetry		
HF	SBKJ/6-31G(d)	2.018	1.005−1.025
MP2[a]	SBKJ/6-31G(d)	1.957	1.020−1.048
BLYP	SBKJ/6-31G(d)	2.027	1.029−1.068
B3LYP	SBKJ/6-31G(d)	2.003	1.021−1.056
PBE0	SBKJ/6-31G(d)	1.974	1.019−1.056
OPBE	SBKJ/6-31G(d)	1.980	1.021−1.065
	(iii) $Co(NH_3)_6 \cdot Cl_4^{-}$, C_3 Symmetry		
HF	SBKJ/6-31G(d)	2.007,[c] 2.002[c]	1.003−1.015
MP2[a]	SBKJ/6-31G(d)	1.947,[c] 1.938[c]	1.018−1.034
MP2[b]	SBKJ/6-31G(d)	1.936,[c] 1.927[c]	1.018−1.034
CAS-SCF(10/10)	SBKJ/6-31G(d)	1.996,[c] 1.989[c]	1.003−1.014
BLYP	SBKJ/6-31G(d)	2.011,[c] 2.003[c]	1.028−1.048
B3LYP	SBKJ/6-31G(d)	1.991,[c] 1.983[c]	1.019−1.036
PBE	SBKJ/6-31G(d)	1.982,[c] 1.975[c]	1.027−1.048
PBE0	SBKJ/6-31G(d)	1.965,[c] 1.958[c]	1.018−1.040
OPBE	SBKJ/6-31G(d)	1.969,[c] 1.962[c]	1.020−1.049
	(iv) $Co(NH_3)_6^{3+}$ in Aqueous Solution[d]		
HF	SBKJ/6-31G(d)	1.998	1.005
PBE	SBKJ/6-31G(d)	1.976	1.029
PBE0	SBKJ/6-31G(d)	1.960	1.019−1.020
OPBE	SBKJ/6-31G(d)	1.967	1.021−1.022
OLYP	SBKJ/6-31G(d)	1.992	1.022−1.023

[a] The 1s levels of N and the 3s/p levels of Co were treated as frozen cores. [b] The 1s levels of N were treated as frozen cores. [c] 3 symmetry equivalent bonds. [d] Hydration modeled using the polarizable continuum model (PCM).

D_{3d} symmetry and is strongly anisotropic (Figure 1). The two added anions give rise to a reduction of the Co−N bonds by 0.03−0.04 Å. The most accurate Co−N bonds (PBE0 and OPBE data) are still too long by ∼0.02 Å compared with the crystal structure data. In the $Co(NH_3)_6 \cdot Cl_4^{-}$ model compound with C_3 symmetry (Table 2iii), the chloride ions form approximately a tetrahedron surrounding the $Co(NH_3)_6^{3+}$ pseudo-octahedron (Figure 2). This model complex is less anisotropic than $Co(NH_3)_6 \cdot Cl_2^{+}$. In $Co(NH_3)_6 \cdot Cl_4^{-}$, the Co−N bond lengths computed with PBE0 and OPBE agree with those of the crystal structures, and therefore this model complex can be considered as acceptable for crystals containing the $Co(NH_3)_6^{3+}$ ion.

In aqueous solution, modeled by the polarizable continuum model (PCM), the Co−N bonds (PBE0 and OPBE data) are as in the $Co(NH_3)_6 \cdot Cl_4^{-}$ model compound (Table 2iv). At least as the geometries are concerned, the water solvent exerts a similar effect on the $Co(NH_3)_6^{3+}$ ion as the lattice anions in the crystals.

Vertical Transitions. The vertical transition energies were computed based on various ground state geometries to probe their sensitivity to the Co−N bond lengths and the environment of the cation (Table 3). At the HF geometry of the free ion, yielding by ∼0.08 Å too long Co−N bonds, the LF transition energies are too low because of the too small crystal-field splitting parameter (Δ). For Co−N bonds fixed at the experimental value, the first singlet−singlet and singlet−triplet transitions, $^1T_{1g} \leftarrow {}^1A_{1g}$ and $^3T_{1g} \leftarrow {}^1A_{1g}$, agree with experiment,[1] but the second transitions, $^1T_{2g} \leftarrow {}^1A_{1g}$ and $^3T_{2g} \leftarrow {}^1A_{1g}$, are underestimated by ∼0.2 eV, and the singlet-quintet $^5T_{2g} \leftarrow {}^1A_{1g}$ transition energy is too low by ∼0.3 eV. Hydration, modeled with PCM, causes a small reduction (∼0.02 eV) of the transition energies. The augmentation of the basis set (from doubleζ + polarization to tripleζ + polarization) yields somewhat lower transition energies. The data based on the MP2 geometry is slightly worse because of the longer Co−N bonds (compared with experiment).

The transition energies based on the HF geometry of $Co(NH_3)_6 \cdot Cl_2^{+}$ are also too low (Table 3iii). The agreement with experiment is better for the more accurate MP2 geometry. For the best geometry (OPBE) based on the best model ($Co(NH_3)_6 \cdot Cl_4^{-}$), the $^1T_{2g} \leftarrow {}^1A_{1g}$, $^3T_{1g} \leftarrow {}^1A_{1g}$, and $^3T_{2g} \leftarrow {}^1A_{1g}$ transition energies agree with experiment, but the $^1T_{1g} \leftarrow {}^1A_{1g}$ energy is overestimated by 0.26 eV (Table 3iv).

The transition energies reported in Table 3 correspond to averages of A and E states because the symmetries of $Co(NH_3)_6^{3+}$, $Co(NH_3)_6 \cdot Cl_2^{+}$, and $Co(NH_3)_6 \cdot Cl_4^{-}$ are lower than O_h (Table 4). A reduction of the symmetry from O_h to D_3 (or D_{3h}) causes a splitting of the T_{1g} and T_{2g} states into $A_2 + E$ (or $A_{2g} + E_g$) and $A_1 + E$ (or $A_{1g} + E_g$) states, respectively. In C_3 symmetry both terms, T_{1g} and T_{2g}, split into A + E. In the $Co(NH_3)_6^{3+}$ ion, the $A_{1/2}$−E splittings are small (0.01 eV), unlike in $Co(NH_3)_6 \cdot Cl_2^{+}$, where the two anions are located in axial positions (Figure 1). This anisotropy causes the larger $A_{1/2}$−E splittings. In contrast to $Co(NH_3)_6^{3+}$, where the $A_{1/2}$ states exhibit slightly lower energies than their corresponding E states, the $A_{1/2}$ energies are higher for $Co(NH_3)_6 \cdot Cl_2^{+}$. Because of the large $A_{1g}-E_g$ splitting of the $^5T_{2g}$ state, $Co(NH_3)_6 \cdot Cl_2^{+}$ is a poor model which is not considered further. The splittings of the singlet and triplet states in $Co(NH_3)_6 \cdot Cl_4^{-}$ are comparable to those of $Co(NH_3)_6 \cdot Cl_2^{+}$, but for $^5T_{2g}$, the A−E splitting is small.

In Table 5 are summarized the vertical transition energies of $Co(NH_3)_6^{3+}$ in the idealized O_h symmetry as well as in the effective D_3 symmetry (Computational Details). Spitting due to spin−orbit (SO) coupling, treated in the D_3* double group, is small (Table 5). The corresponding data for $Co(NH_3)_6 \cdot Cl_4^{-}$ is given in Table 6; the splittings due to spin−orbit coupling are as for $Co(NH_3)_6^{3+}$ but, as already mentioned, the transition energies are higher and more accurate (Table 3). On the basis of the $Co(NH_3)_6^{3+}$ and $Co(NH_3)_6 \cdot Cl_4^{-}$ models, the $^5T_{2g}$ energy is higher than those of the triplet states and lower than those of the singlets.

Table 3. Vertical Ligand-Field Transition Energies[a] of $Co(NH_3)_6^{3+}$

geometry	basis set	$^1T_{1g} \leftarrow {}^1A_{1g}$	$^1T_{2g} \leftarrow {}^1A_{1g}$	$^3T_{1g} \leftarrow {}^1A_{1g}$	$^3T_{2g} \leftarrow {}^1A_{1g}$	$^5T_{2g} \leftarrow {}^1A_{1g}$
		(i) Experimental Data[b]				
		2.60	3.66	1.61	2.14[c]	
		(ii) $Co(NH_3)_6^{3+}$, D_3 Symmetry				
HF	SBKJ/6-31G(d)	2.21	2.96	0.85	1.36	1.21
HF[d]	SBKJ/6-31G(d)	2.66, 2.63[e]	3.48, 3.45[e]	1.36, 1.34[e]	1.93, 1.90[e]	2.14, 2.12[e]
HF[d]	SBKJ/6-311G(d)	2.64	3.45	1.35	1.90	2.10
HF[d]	SBKJu/6-311G(d)	2.59	3.37	1.31	1.86	2.09
MP2[f]	SBKJ/6-31G(d)	2.51	3.31	1.21	1.75	1.86
MP2[f]	SBKJ/6-311G(d)	2.53	3.32	1.22	1.76	1.88
		(iii) $Co(NH_3)_6 \cdot Cl_2^+$, D_{3d} Symmetry				
HF	SBKJ/6-31G(d)	2.46	3.19	1.13	1.62	1.68
MP2[f]	SBKJ/6-31G(d)	2.80	3.58	1.51	2.04	2.32
		(iv) $Co(NH_3)_6 \cdot Cl_4^-$, C_3 Symmetry				
OPBE	SBKJ/6-31G(d)	2.86	3.60	1.57	2.07	2.46

[a] Units: eV. [b] Reference 4. [c] Calculated[44] according to Tanabe and Sugano.[45] [d] d(Co−N) fixed at 1.96 Å. [e] With PCM hydration. [f] The 1s levels of N and the 3s/p levels of Co were treated as frozen cores.

Table 4. A_1-E and A_2-E or $A-E$ Splittings[a] of the T_{2g} and T_{1g} States

geometry	basis set	$^1T_{1g}$	$^1T_{2g}$	$^3T_{1g}$	$^3T_{2g}$	$^5T_{2g}$
		(i) $Co(NH_3)_6^{3+}$, D_3 Symmetry				
HF	SBKJ/6-31G(d)	4.18	8.95	1.88	6.39	3.11
HF[b]	SBKJ/6-31G(d)	4.33, 4.54[c]	11.3, 11.3[c]	2.50, 2.58[c]	8.08, 8.18[c]	4.63, 5.39[c]
HF[b]	SBKJ/6-311G(d)	4.49	10.2	2.34	8.00	5.82
HF[b]	SBKJu/6-311G(d)	4.49	9.25	2.78	8.14	5.82
MP2[d]	SBKJ/6-31G(d)	4.14	8.41	3.10	6.69	6.01
MP2[d]	SBKJ/6-311G(d)	4.41	8.76	3.21	7.07	6.34
		(ii) $Co(NH_3)_6 \cdot Cl_2^+$, D_{3d} Symmetry				
HF	SBKJ/6-31G(d)	36.2	36.5	29.5	41.1	92.1
MP2[d]	SBKJ/6-31G(d)	55.3	44.5	42.7	50.9	270
		(iii) $Co(NH_3)_6 \cdot Cl_4^-$, C_3 Symmetry				
OPBE	SBKJ/6-31G(d)	14.7	55.7	46.3	38.4	4.7

[a] Units: meV. [b] (Co−N) fixed at 1.96 Å. [c] With PCM hydration. [d] The 1s levels of N and the 3s/p levels of Co were treated as frozen cores.

TDDFT based on the BLYP and B3LYP functionals overestimates the (vertical) LF transitions energies (Table S6).

0−0 Transitions. Their computation requires optimized excited state geometries. Because of the Jahn−Teller theorem, the degeneracy is removed and hence these geometries were computed with the OPBE functional and PCM hydration (OPBE-PCM), since this method reproduced the Co−N bond lengths of the $Co(NH_3)_6^{3+}$ ion in the crystal structures (Tables 1 and 2iv). All of these PCM computations had to be performed in C_1 symmetry. Attempts to optimize the geometries of the excited states of the $Co(NH_3)_6 \cdot Cl_4^-$ model compound were unsuccessful. The computed Co−N bond lengths of the ground state and the excited $^1T_{1g}$, $^3T_{1g}$, and $^5T_{2g}$ states are reported in Table 7. In the $^1T_{1g}$ and $^3T_{1g}$ states, the spatial MO occupations are virtually equal, and this is the reason why their geometries differ only marginally. In agreement with Wilson and Solomon's study,[1] these two states exhibit a compressed octahedral structure with a computed shortening of the axial bonds of 0.010 and 0.014 Å for the $^3T_{1g}$ and $^1T_{1g}$ states, respectively, and an elongation of the equatorial bonds of ∼0.15 Å. This data agrees well with the spectroscopically determined[1] values of ∼0.02 (compression) and ∼0.12 Å (elongation). The geometry of the $^5T_{2g}$ state is almost octahedral. In this state, the Co−N bond lengths are elongated by ∼0.17 Å with respect to those

Table 5. Computed Vertical Ligand-Field Transition Energies[a] of $Co(NH_3)_6^{3+}$ Including Spin-Orbit Coupling

O_h	D_3	D_3^*
0.0000 ($^1A_{1g}$)	0.0000 ($^1A_1$)	0.0000 (A_1)
1.36 ($^3T_{1g}$)	1.3608 (^3E)	1.4118 (A_1)
	1.3583 ($^3A_2$)	1.3819 (A_2)
		1.3797 (E)
		1.3402 (E)
		1.3388 (E)
		1.3387 (A_1)
1.93 ($^3T_{2g}$)	1.9327 (^3E)	1.9880 (A_2)
	1.9246 ($^3A_1$)	1.9783 (A_1)
		1.9755 (E)
		1.9531 (E)
		1.9497 (E)
		1.9480 (A_2)
2.14 ($^5T_{2g}$)	2.1415 (^5E)	2.2009 (A_1)
	2.1369 ($^5A_1$)	2.1961 (A_2)
		2.1942 (E)
		2.1897 (A_1)
		2.1895 (E)
		2.1269 (E)
		2.1231 (A_2)
		2.1220 (E)
		2.0934 (E)
		2.0933 (A_1)
2.66 ($^1T_{1g}$)	2.6614 (^1E)	2.6756 (E)
	2.6571 ($^1A_2$)	2.6728 (A_2)
3.48 ($^1T_{2g}$)	3.4838 (^1E)	3.4948 (E)
	3.4725 ($^1A_1$)	3.4830 (A_1)

[a] Units: eV; HF/SBKJ/6-31G(d) geometry with C−N bond lengths of 1.96 Å.

Table 6. Computed Vertical Ligand-Field Transition Energies[a] of $Co(NH_3)_6 \cdot Cl_4^-$ Including Spin-Orbit Coupling

O_h	C_3	C_3*
0.00 ($^1A_{1g}$)	0.0000 (^1A)	0.0000 (A)
1.57 ($^3T_{1g}$)	1.5869 (^3E)	1.6004 (A)
	1.5406 (^3A)	1.5736 (A)
		1.5665 (E)
		1.5292 (E)
		1.5252 (E)
		1.5246 (A)
2.07 ($^3T_{2g}$)	2.0795 (^3E)	2.1267 (A)
	2.0411 (^3A)	2.1194 (E)
		2.0988 (E)
		2.0983 (A)
		2.0008 (E)
		1.9955 (A)
2.46 ($^5T_{2g}$)	2.4643 (^5E)	2.5207 (A)
	2.4596 (^5A)	2.5166 (A)
		2.5141 (E)
		2.5101 (A)
		2.5098 (E)
		2.4466 (E)
		2.4423 (E)
		2.4402 (A)
		2.4142 (A)
		2.4134 (E)
2.86 ($^1T_{1g}$)	2.8669 (^1E)	2.8762 (E)
	2.8522 (^1A)	2.8678 (A)
3.60 ($^1T_{2g}$)	3.6193 (^1E)	3.6381 (E)
	3.5637 (^1A)	3.5740 (A_1)

[a] Units: eV.

Table 7. Co−N Bond Lengths in the $^1A_{1g}$, $^1T_{1g}$, $^3T_{1g}$, and $^5T_{2g}$ States of $Co(NH_3)_6^{3+}$

state	d(Co−N), Å	remarks
$^1A_{1g}$	1.967[a]	D_3 symmetry, (pseudo)octahedron
$^1T_{1g}$	1.953, 1.953, 2.098, 2.098, 2.123, 2.128	compressed (pseudo)octahedron
$^3T_{1g}$	1.957, 1.957, 2.099, 2.100, 2.124, 2.129	compressed (pseudo)octahedron
$^5T_{2g}$	2.129, 2.130, 2.138, 2.138, 2.139, 2.139	∼ regular (pseudo)octahedron

[a] Six symmetry-equivalent Co−N bonds.

Table 8. 0−0 Transition Energies (ΔE)

		ΔE_{calc}, eV		
state	ΔE_{exp},[a] eV	MCQDPT2[b]	OPBE	E_{SO}, cm^{-1}
$^1A_{1g}$				−76.9
$^1T_{1g}$	2.36	2.36 (2.62)	1.70	−10.0
$^3T_{1g}$	1.37	0.95 (1.33)	1.20	−78.6
$^5T_{2g}$		1.60 (2.12)	1.82	−51.7

[a] Reference 1. [b] In parentheses: vertical transitions.

in the $^1A_{1g}$ ground state. A smaller elongation of ∼0.12 Å was estimated by Wilson and Solomon.[1]

The 0−0 transition energies (Table 8) were computed with multiconfiguration quasidegenerate second-order perturbation (MCQDPT2)[16,17] theory and density functional theory using the OPBE functional. These calculations were based on the above-described OPBE-PCM geometries (Table 7). PCM hydration was included to model the effect of the environment of $Co(NH_3)_6^{3+}$. Contributions from spin−orbit coupling (E_{SO}) were taken into account, but they are small (Table 8). E_{SO} was obtained via spin−orbit CI (Computational Details), which was based on the CAS-SCF wave function of the corresponding state including the interactions with other states of appropriate symmetry and spin (Computational Details). Zero point energy corrections were not included because they would be questionable: as mentioned above, it was not possible to optimize the geometries of the excited states of the $Co(NH_3)_6 \cdot Cl_4^-$ model compound. Hence, hydrogen bonding of ammonia with lattice anions could not be treated (see above). The neglect of these H-bonds gives rise to low-frequency rotational modes of the ammonia ligands. In the presence of anions and, therefore, H-bonds, these modes would have much higher frequencies. The MCQDPT2 energy of the $^1T_{1g}$ state agrees with experiment, but that of the $^3T_{1g}$ state is too low by 0.32 eV. Interestingly, the OPBE $^3T_{1g}$ energy is underestimated by only 0.17 eV, but that of $^1T_{1g}$ is inaccurate and too low by 0.66 eV. For the experimentally unknown $^5T_{2g}$ state, the MCQDPT2 and OPBE energies differ by 0.22 eV. On the basis of the more reliable MCQDPT2 energies, the $^5T_{2g}$ state lies above the $^3T_{1g}$ state by 0.65 eV and below the $^1T_{1g}$ state. According to the OPBE energies, which are less reliable, the $^5T_{2g}$ state lies also above the $^3T_{1g}$ state by 0.62 eV, but the $^1T_{1g}$ energy (which deviates strongly from the experimental value) is lower than that of the $^5T_{2g}$ state. The lowest (relaxed) excited state of $Co(NH_3)_6^{3+}$ is the triplet $^3T_{1g}$ state and not the quintet $^5T_{2g}$ state. The vertical transition energies, calculated without chloride ions in the second coordination sphere, were too low by ∼0.2−0.3 eV (Table 3). Possibly, the 0−0 transition energies (Table 8) are also too low by this error.

Table 9. Experimental and Computed Symmetric Stretching Frequencies of $Co(NH_3)_6^{3+}$[a]

	a_{1g}		e_g	
state	exptl[b]	calcd	exptl[b]	calcd
$^1A_{1g}$	490	458, 460[c]	440	425,[d] 426[c]
$^1T_{1g}$	480	454	429	371, 184
$^3T_{1g}$	483	447	434	373, 151
$^5T_{2g}$	∼435[e]	382	-	304[d]

[a] OPBE-PCM geometries, unless noted otherwise. Units: cm^{-1}. [b] Reference 1. [c] $Co(NH_3)_6 \cdot Cl_4^-$ model compound. [d] Average of the two e_g components. [e] Estimated.

Vibrational Frequencies. For the $^1A_{1g}$ ground state, the vibrational frequencies were computed based on the $Co(NH_3)_6^{3+}$ OPBE-PCM and the $Co(NH_3)_6 \cdot Cl_4^-$ OPBE (gas phase) geometries. The computed frequencies are insensitive to the model (Table 9) and lower than the experimental values. The frequencies of the excited $^1T_{1g}$ and $^3T_{1g}$ states are also underestimated, whereby the error of the e_g component is sizable, possibly because the distortion of the PCM geometries is larger than those of $Co(NH_3)_6^{3+}$ in the solid, where the motion of the nearest neighbors is restricted. Assuming an average error of −31 cm^{-1} for the a_{1g} component, the best estimate of the a_{1g} mode for the $^5T_{2g}$ state would be ∼413 cm^{-1}, being somewhat lower than the value estimated from experiment. This difference might again be due to the full relaxation of the PCM geometry.

Discussion

Quantum Chemical Investigations of the Related Low-Spin $Co(CN)_6^{3-}$ and $Co(OH_2)_6^{3+}$Complexes. The vertical LF transitions of the low-spin $Co(CN)_6^{3-}$ ion have been computed[46] at the experimental geometry using DFT-

Table 10. Vertical Ligand Field Transition Energies of $Co(OH_2)_6^{3+}$

electronic state	$Co(OH_2)_6^{3+}$			$Co(OH_2)_6 \cdot (OH_2)_{12}^{3+}$	
	LFDFT[a]	SORCI[a]	TDDFT[a]	LFDFT[a]	exp.[b]
$^1A_{1g}$	0	0	0	0	0
$^1T_{1g}$	15370	15670	16528	15669	16500
$^1T_{2g}$	24537	23600	22017	24726	24700
$^3T_{1g}$	9212	5257	9156	10271	8000
$^3T_{2g}$	13782	10779	9380	14798	12500
$^5T_{2g}$	9660			12649	

[a] From ref 46. [b] From ref 44.

based LF theory (LFDFT)[47] and the spectroscopically oriented configuration interaction method (SORCI).[48] The agreement with experiment is better for the SORCI technique. For the $Co(OH_2)_6^{3+}$ ion (Table 10), the transition energies, computed at the experimental Co−N bond lengths, were taken from Table 19-7 of ref 46 in which the experimental data has been replaced by those of Johnson and Sharpe,[44] who measured transition energies to the singlet and the triplet states. All of the applied methods agree with experiment, whereby it should be noted that SORCI underestimates the $^3T_{1g}$ energy by further 0.1 eV than MCQDPT2 for $Co(NH_3)_6^{3+}$ (Table 3). For $Co(CN)_6^{3-}$ and $Co(OH_2)_6^{3+}$, energies computed with CAS-SCF-based second-order perturbation theory is not available. Environmental effects were not modeled; they were assumed to cancel largely.

The above-mentioned LFDFT and SORCI vertical transition energies agree with experiment because (i) these calculations were performed at the experimental cobalt(III)−ligand bond lengths, and (ii) because systematic errors due to the neglect of environmental effects cancel largely. It should be noted that LF theory is based on the Racah parameters Δ, B, and C, whose expressions are derived from Coulomb and exchange integrals, whereby electron correlation energy is accounted for in an effective, nonspecific way. Since Δ, B, and C are obtained via a fit to experimental data, the errors arising from the approximate treatment of electron correlation cancel partially. The computation of 0−0 transitions is more demanding, since accurate geometries of ground and excited states are required. Because of the differences in metal−ligand bond lengths of ground and excited states, the Coulomb and exchange integrals vary. The parameters Δ, B, and C are not constant for 0−0 transitions, and the error arising from the neglect of electron correlation is different than for vertical transitions. Therefore, 0−0 transitions predicted by LF theory cannot be expected to be accurate, and energies of the relaxed $^5T_{2g}$ states of $Co(OH_2)_6^{3+}$ and $Co(NH_3)_6^{3+}$, estimated on the basis of LF theory, are likely to be affected by those systematic errors.

Geometry of the $Co(NH_3)_6^{3+}$ Ion. The Co−N bond lengths computed with MP2 for the free $Co(NH_3)_6^{3+}$ ion are close to those in the crystal structures (Tables 1 and 2i). However, the MP2 geometry is not correct, since static electron correlation is neglected, and since the gas phase geometry is expected to differ form those in the crystal. In aqueous solution and in crystals, the Co−N bonds are shorter than in the free ion because charge transfer from solvent molecules or anions to the cation strengthens the Co−N bonds. The electronic transition energies in $Ru(NH_3)_6^{2+}$ and $Ru(NH_3)_5(pyr)^{2+}$ (pyr: pyridine) were shown to depend strongly on the solvent-to-solute charge transfer.[49] According to QM/MM computations[49] on these Ru^{II} and Ru^{III} complexes, roughly one electron is transferred from the water solvent to the $Ru(NH_3)_6^{2+/3+}$ and $Ru(NH_3)_5(pyr)^{2+/3+}$ ions. The neglect of this solvent-to-solute charge transfer effect in quantum chemical computations on di- and trivalent cations is responsible for the systematically too long metal−ligand bond lengths. It is interesting to note that PCM, which takes into account electrostatic solute−solvent interactions (the hydrogen bonds are mainly electrostatic) provides Co−N bond lengths being close to those in the crystal structures.

Transition Energies. Experimentally, the $^5T_{2g}$ energy has not been measurable so far. According to ZINDO calculations of Larsson, Ståhl, and Zerner,[2] the vertical $^5T_{2g}$ energy is higher than that of the $^3T_{1g}$, $^3T_{2g}$, and $^1T_{1g}$ states, and lower than that of the $^1T_{2g}$ state. The present calculations suggest that the $^5T_{2g}$ energy is higher than those of the two triplets, and lower than those of the two singlets. The comparison with experimentally available transition energies shows that the computational error is $\leq$0.3 eV (Table 3iv). Because of this error, the present computations do not allow the assessment of the $^5T_{2g}-{}^1T_{1g}$ ordering. However, there is little doubt that the (vertical) $^5T_{2g}$ energy is higher than those of the $^3T_{1g}$ and $^3T_{2g}$ states.

The 0−0 transition energies, computed on the basis of the ZINDO method,[2] increase in the order $^3T_{1g} < {}^1T_{1g} \approx {}^5T_{2g}$. According to the spectroscopic study,[1] the energy ordering is $^5T_{2g} \leq {}^3T_{1g} < {}^1T_{1g}$, and the present computations suggest the ordering $^3T_{1g} < {}^5T_{2g} < {}^1T_{1g}$. The computed $^1T_{1g}$ energy agrees with experiment, but the $^3T_{1g}$ energy is too low by 0.42 eV (Table 8). Because of the magnitude of the $^5T_{2g}-{}^3T_{1g}$ energy difference (Table 8) the statement that the $^5T_{2g}$ energy is higher than the $^3T_{1g}$ energy can be made with confidence. Because of the sizable error in the $^3T_{1g}$ energy, however, the question, whether the $^5T_{2g}$ state lies below the $^1T_{1g}$ state or whether their energies are comparable, remains open. It should be remembered that it was not possible to optimize the geometries of the $^1T_{1g}$, $^3T_{1g}$, and $^5T_{2g}$ states for the $Co(NH_3)_6 \cdot Cl_4^-$ model. Hence, the 0−0 transition energies based on the best model are not available. The environment of the $Co(NH_3)_6^{3+}$ ion had to be represented with PCM water. It should be noted that the geometries of the excited states, computed at the OPBE-PCM level, are fully relaxed. It is an open question, whether in the crystal the excited states can relax completely, since the motion of the lattice anions is restricted. These constraints would also affect the relaxation of the Co−N bonds. The longer Co−N bonds and the lower vibrational frequencies for the computed excited states compared with Wilson et al.'s experimental data in the solid state might also be due to a possible incomplete relaxation in the crystal (whereby inaccuracies in the computations contribute as well). In contrast to $Co(NH_3)_6^{3+}$, for $Co(OH_2)_6^{3+}$, exhibiting a weaker crystal field, the $^5T_{2g}$ state is the lowest excited 0−0 state.[50]

Acknowledgment. I am grateful to Dr. M. W. Schmidt for a nonpublic version of GAMESS.

Supporting Information Available: Tables S1−S4 listing the atomic coordinates of hydrated $Co(NH_3)_6^{3+}$ in its $^1A_{1g}$, $^1T_{1g}$, $^3T_{1g}$, and $^5T_{2g}$ states, Table S5 listing the atomic coordinates of $Co(NH_3)_6 \cdot Cl_4^-$ in the ground state, and Table S6 summarizing the vertical LF transition energies obtained with TDDFT (BLYP and B3LYP). This material is available free of charge via the Internet at http://pubs.acs.org.

References

(1) Wilson, R. B.; Solomon, E. I. *J. Am. Chem. Soc.* **1980**, *102*, 4085.

(2) Larsson, S.; Ståhl, K.; Zerner, M. C. *Inorg. Chem.* **1986**, *25*, 3033.

(3) McCusker, J. K.; Walda, K. N.; Magde, D.; Hendrickson, D. N. *Inorg. Chem.* **1993**, *32*, 394.

(4) Konya, K.; Nishikawa, H.; Shibata, M. *Inorg. Chem.* **1968**, *7*, 1165.

(5) Schmidt, M. W.; Baldridge, K. K.; Boatz, J. A.; Elbert, S. T.; Gordon, M. S.; Jensen, J. H.; Koseki, S.; Matsunaga, N.; Nguyen, K. A.; Su, S. J.; Windus, T. L.; Dupuis, M.; Montgomery, J. A. *J. Comput. Chem.* **1993**, *14*, 1347.

(6) Gordon, M. S.; Schmidt, M. W., In *Theory and Applications of Computational Chemistry, the first forty years*; Dykstra, C. E.; Frenking, G.; Kim, K. S.; Scuseria, G. E. Eds.; Elsevier: Amsterdam, 2005, pp 1167−1189.

(7) Stevens, W. J.; Krauss, M.; Basch, H.; Jasien, P. G. *Can. J. Chem.* **1992**, *70*, 612.

(8) Stevens, W. J.; Basch, H.; Krauss, M. *J. Chem. Phys.* **1984**, *81*, 6026.

(9) Schäfer, A.; Horn, H.; Ahlrichs, R. *J. Chem. Phys.* **1992**, *97*, 2571.

(10) Hehre, W. J.; Ditchfield, R.; Pople, J. A. *J. Chem. Phys.* **1972**, *56*, 2257.

(11) Ditchfield, R.; Hehre, W. J.; Pople, J. A. *J. Chem. Phys.* **1971**, *54*, 724.

(12) Krishnan, R.; Binkley, J. S.; Seeger, R.; Pople, J. A. *J. Chem. Phys.* **1980**, *72*, 99.

(13) Bode, B. M.; Gordon, M. S. *J. Mol. Graphics Modell.* **1998**, *16*, 133.

(14) Tomasi, J. *Theor. Chem. Acc.* **2004**, *112*, 184.

(15) Tomasi, J.; Mennucci, B.; Cammi, R. *Chem. Rev.* **2005**, *105*, 2999.

(16) Nakano, H. *J. Chem. Phys.* **1993**, *99*, 7983.

(17) Nakano, H. *Chem. Phys. Lett.* **1993**, *207*, 372.

(18) Rotzinger, F. P. *J. Phys. Chem. B* **2005**, *109*, 1510.

(19) Rotzinger, F. P. *J. Phys. Chem. A* **1999**, *103*, 9345.

(20) Furlani, T. R.; King, H. F. *J. Chem. Phys.* **1985**, *82*, 5577.

(21) King, H. F.; Furlani, T. R. *J. Comput. Chem.* **1988**, *9*, 771.

(22) Fedorov, D. G.; Gordon, M. S. *J. Chem. Phys.* **2000**, *112*, 5611.

(23) Seitz, K.; Peschel, S.; Babel, D. *Z. Anorg. Allg. Chem.* **2001**, *627*, 929.

(24) Iwata, M.; Saito, Y. *Acta Crystallogr. B* **1973**, *29*, 822.

(25) Barnet, M. T.; Craven, B. M.; Freeman, H. C. *J. Chem. Soc., Chem. Commun.* **1966**, 307.

(26) Meek, D. W.; Ibers, J. A. *Inorg. Chem.* **1970**, *9*, 465.

(27) Beattie, J. K.; Moore, C. J. *Inorg. Chem.* **1982**, *21*, 1292.

(28) Schroeder, D. R.; Jacobson, R. A. *Inorg. Chem.* **1973**, *12*, 210.

(29) Schroeder, D. R.; Jacobson, R. A. *Inorg. Chem.* **1973**, *12*, 515.

(30) Sharma, R. P.; Bala, R.; Sharma, R.; Perez, J.; Miguel, D. *J. Mol. Struct.* **2006**, *788*, 49.

(31) Sharma, R. P.; Bala, R.; Sharma, R.; Venugopalan, P.; Salas, J. M.; Quiros, M. *J. Fluorine Chem.* **2005**, *126*, 1543.

(32) Sharma, R. P.; Bala, R.; Sharma, R.; Rychlewska, U.; Warzajtis, B. *J. Fluorine Chem* **2005**, *126*, 967.

(33) Becke, A. D. *Phys. Rev. A* **1988**, *38*, 3098.

(34) Lee, C.; Yang, W.; Parr, R. G. *Phys. Rev. B* **1988**, *3*, 7–785.

(35) Miehlich, B.; Savin, A.; Stoll, H.; Preuss, H. *Chem. Phys. Lett.* **1989**, *157*, 200.

(36) Becke, A. D. *J. Chem. Phys.* **1993**, *9*, 8–5648.

(37) Stephens, P. J.; Devlin, F. J.; Chablowski, C. F.; Frisch, M. J. *J. Phys. Chem.* **1994**, *98*, 11623.

(38) Hertwig, R. H.; Koch, W. *Chem. Phys. Lett.* **1997**, *268*, 345.

(39) Perdew, J. P.; Burke, K.; Ernzerhof, M. *Phys. Rev. Lett.* **1996**, *77*, 3865.

(40) Perdew, J. P.; Burke, K.; Ernzerhof, M. *Phys. Rev. Lett.* **1997**, *78*, 1396.

(41) Adamo, C.; Barone, V. *J. Chem. Phys.* **1999**, *110*, 6158.

(42) Handy, N. C.; Cohen, A. J. *Mol. Phys.* **2001**, *99*, 403.

(43) Conradie, J.; Ghosh, A. *J. Phys. Chem. B* **2007**, *111*, 12621.

(44) Johnson, D. A.; Sharpe, A. G. *J. Chem. Soc. A* **1966**, 798.

(45) Tanabe, Y.; Sugano, S. *J. Phys. Soc. Jpn.* **1954**, *9*, 753.

(46) Atanasov, M.; Comba, P.; Daul, C. A.; Neese, F. In *Models, Mysteries and Magic of Molecules*; Boeyens, J. C. A.; Ogilvie, J. F., Eds.; Springer: Dordrecht, 2008; pp 411−445.

(47) Atanasov, M.; Daul, C. A.; Rauzy, C. *Struct. Bonding (Berlin)* **2004**, *106*, 97.

(48) Neese, F. *J. Chem. Phys.* **2003**, *119*, 9428.

(49) Pearl, G. M.; Zerner, M. *J. Am. Chem. Soc.* **1999**, *121*, 399.

(50) Johnson, D. A.; Nelson, P. G. *Inorg. Chem.* **1999**, *38*, 4949.

CT900048R